Table S1. Crystal data and structure refinement details for **1**.

Empirical formula	$C_{12}H_{17}Br_4MnN_3O_2$
Formula weight	609.86
Temperature/K	150.00
Crystal system	monoclinic
Space group	$P2_1/c$
a/Å	16.6627(4)
b/Å	7.8392(2)
c/Å	15.8449(4)
α/°	90
β/°	108.6470(10)
γ/°	90
Volume/Å^3	1961.05(9)
Z	4
ρ_{calc}g/cm^3	2.066
μ/mm^{-1}	8.830
F(000)	1164.0
Crystal size/mm^3	0.14 × 0.1 × 0.08
Radiation	MoKα (λ = 0.71073)
2Θ range for data collection/°	5.16 to 61.078
Index ranges	$-23 \le h \le 23$, $-11 \le k \le 11$, $-22 \le l \le 19$
Reflections collected	27218
Independent reflections	5998 [R_{int} = 0.0409, R_{sigma} = 0.0370]
Data/restraints/parameters	5998/2/208
Goodness-of-fit on F^2	1.060
Final R indexes [I>=2σ (I)]	R_1 = 0.0268, wR_2 = 0.0503
Final R indexes [all data]	R_1 = 0.0418, wR_2 = 0.0536
Largest diff. peak/hole / e Å^{-3}	0.53/-0.47

Table S2. Fractional Atomic Coordinates (×10^4) and Equivalent Isotropic Displacement Parameters (Å^2×10^3) for **1**. U_{eq} is defined as 1/3 of the trace of the orthogonalised U_{IJ} tensor.

Atom	x	y	z	U(eq)
Br4	6696.2(2)	9862.5(2)	9102.9(2)	23.62(6)
Br3	7269.3(2)	5058.7(3)	9633.3(2)	27.67(6)
Br1	8555.3(2)	8056.0(3)	8229.2(2)	30.01(6)
Br2	6147.4(2)	6546.6(3)	6995.6(2)	36.39(7)
Mn1	7192.8(2)	7250.1(4)	8462.7(2)	21.58(8)
O1	7951.8(10)	3719.2(19)	6058.8(10)	27.2(4)
O2	8105.0(13)	6890(2)	6157.0(12)	34.1(4)
N1	8006.3(11)	3262(2)	6913.0(11)	20.4(4)
N2	7659.4(12)	2261(2)	8001.1(12)	23.1(4)
N3	6284.8(11)	2809(2)	5685.4(11)	21.6(4)
C1	7353.7(14)	2606(2)	7121.4(14)	19.8(4)
C8	6493.8(13)	2335(2)	6547.5(13)	19.3(4)
C9	5869.6(15)	1636(3)	6839.9(15)	28.0(5)
C11	4862.3(14)	1999(3)	5384.7(15)	26.8(5)
C3	8721.5(14)	3335(3)	7634.7(14)	22.2(4)
C2	8498.8(14)	2690(3)	8325.9(14)	23.9(5)
C12	5496.9(14)	2661(3)	5111.0(15)	25.9(5)
C4	9569.7(14)	3983(3)	7677.0(16)	29.4(5)
C10	5054.2(15)	1468(3)	6259.3(15)	31.2(5)
C5	10094.6(15)	4183(3)	8662.4(17)	36.8(6)

C7	9080.4(15)	2496(3)	9252.3(15)	33.2(6)
C6	9990.8(16)	2667(3)	9228.7(17)	37.8(6)

Table S3. Anisotropic Displacement Parameters ($Å^2×10^3$) for **1**. The Anisotropic displacement factor exponent takes the form: $-2\pi^2[h^2a^{*2}U_{11}+2hka^*b^*U_{12}+\ldots]$.

Atom	U_{11}	U_{22}	U_{33}	U_{23}	U_{13}	U_{12}
Br4	32.83(13)	21.74(10)	19.73(11)	0.28(8)	13.23(10)	4.57(9)
Br3	33.66(14)	21.96(10)	29.15(13)	4.45(9)	12.51(11)	4.13(9)
Br1	25.13(13)	37.27(13)	29.97(13)	-3.58(10)	12.06(10)	2.5(1)
Br2	38.50(15)	39.21(13)	23.42(13)	-7.69(10)	-1.38(11)	4.82(11)
Mn1	24.10(18)	22.33(15)	18.50(17)	-0.91(12)	7.09(14)	3.29(14)
O1	30.6(9)	31.6(8)	21.4(8)	1.6(7)	11.2(7)	-4.1(7)
O2	41.5(11)	35.4(9)	25.4(10)	0.9(8)	10.6(9)	-4.1(8)
N1	22.2(10)	22.7(8)	16.9(9)	1.7(7)	7.3(8)	0.3(7)
N2	24.4(10)	27.1(9)	19.3(9)	2.2(7)	9.2(8)	1.9(8)
N3	20.9(10)	27.8(9)	17.8(9)	0.1(7)	8.4(8)	-5.8(8)
C1	21.3(11)	20.4(9)	18.3(10)	2.0(8)	7.0(9)	3.5(9)
C8	20.2(11)	19.3(9)	19.0(10)	0.6(8)	6.8(9)	2.7(8)
C9	24.8(12)	38.1(12)	21.6(12)	8.7(10)	8.1(10)	0.3(10)
C11	19.1(12)	33.7(12)	25.4(12)	-1.0(9)	3.8(10)	-1.8(10)
C3	19.1(11)	22.6(10)	24.0(11)	-2.5(9)	5.6(9)	2.1(9)
C2	23.8(12)	25.0(10)	20.1(11)	-1.4(9)	2.9(9)	2.9(9)
C12	22.5(12)	34.7(12)	17.9(11)	-0.7(9)	2.6(9)	-3.4(10)
C4	21.3(12)	31.0(12)	36.1(14)	0.0(10)	9.3(10)	1.0(10)
C10	21.4(12)	42.2(13)	31.7(13)	7.3(11)	10.9(10)	-4.1(10)
C5	21.3(13)	42.5(14)	39.3(15)	-6.5(12)	-0.8(11)	3.2(11)
C7	30.7(14)	41.9(13)	22.6(12)	-0.5(10)	2.5(11)	7.4(11)
C6	29.6(14)	45.8(15)	30.3(14)	-2.7(11)	-1.3(11)	12.4(12)

Table S4. Bond Lengths for **1**.

Atom	Atom	Length/Å	Atom	Atom	Length/Å
Br4	Mn1	2.5386(4)	C1	C8	1.446(3)
Br3	Mn1	2.5012(4)	C8	C9	1.380(3)
Br1	Mn1	2.4955(4)	C9	C10	1.382(3)
Br2	Mn1	2.4805(4)	C11	C12	1.367(3)
O1	N1	1.375(2)	C11	C10	1.383(3)
N1	C1	1.336(3)	C3	C2	1.361(3)
N1	C3	1.364(3)	C3	C4	1.483(3)
N2	C1	1.350(3)	C2	C7	1.486(3)
N2	C2	1.369(3)	C4	C5	1.534(3)
N3	C8	1.350(3)	C5	C6	1.532(4)
N3	C12	1.342(3)	C7	C6	1.535(3)

Table S5. Bond Angles for **1**.

Atom	Atom	Atom	Angle/°	Atom	Atom	Atom	Angle/°
Br3	Mn1	Br4	101.749(13)	C9	C8	C1	123.28(19)
Br1	Mn1	Br4	106.455(14)	C8	C9	C10	120.0(2)
Br1	Mn1	Br3	116.791(15)	C12	C11	C10	118.5(2)
Br2	Mn1	Br4	109.443(14)	N1	C3	C4	128.1(2)
Br2	Mn1	Br3	113.342(15)	C2	C3	N1	105.6(2)
Br2	Mn1	Br1	108.475(15)	C2	C3	C4	126.3(2)
C1	N1	O1	122.74(18)	N2	C2	C7	127.7(2)
C1	N1	C3	111.77(18)	C3	C2	N2	107.30(19)

C3	N1	O1	125.43(18)	C3	C2	C7	125.0(2)
C1	N2	C2	109.99(18)	N3	C12	C11	120.4(2)
C12	N3	C8	122.85(19)	C3	C4	C5	107.81(19)
N1	C1	N2	105.31(18)	C9	C10	C11	120.1(2)
N1	C1	C8	128.47(19)	C6	C5	C4	112.5(2)
N2	C1	C8	126.21(19)	C2	C7	C6	107.7(2)
N3	C8	C1	118.62(19)	C5	C6	C7	112.3(2)
N3	C8	C9	118.10(19)				

Table S6. Torsion Angles for **1**.

A	B	C	D	Angle/°	A	B	C	D	Angle/°
O1	N1	C1	N2	177.54(17)	C8	N3	C12	C11	-0.4(3)
O1	N1	C1	C8	-3.5(3)	C8	C9	C10	C11	0.1(4)
O1	N1	C3	C2	-177.07(17)	C3	N1	C1	N2	0.4(2)
O1	N1	C3	C4	3.3(3)	C3	N1	C1	C8	179.39(19)
N1	C1	C8	N3	-1.2(3)	C3	C2	C7	C6	-15.4(3)
N1	C1	C8	C9	179.8(2)	C3	C4	C5	C6	43.2(3)
N1	C3	C2	N2	-0.4(2)	C2	N2	C1	N1	-0.6(2)
N1	C3	C2	C7	179.2(2)	C2	N2	C1	C8	-179.65(19)
N1	C3	C4	C5	166.9(2)	C2	C3	C4	C5	-12.7(3)
N2	C1	C8	N3	177.59(19)	C2	C7	C6	C5	45.9(3)
N2	C1	C8	C9	-1.4(3)	C12	N3	C8	C1	-177.68(19)
N2	C2	C7	C6	164.1(2)	C12	N3	C8	C9	1.4(3)
N3	C8	C9	C10	-1.2(3)	C12	C11	C10	C9	1.0(4)
C1	N1	C3	C2	0.0(2)	C4	C3	C2	N2	179.31(19)
C1	N1	C3	C4	-179.7(2)	C4	C3	C2	C7	-1.1(4)
C1	N2	C2	C3	0.6(2)	C4	C5	C6	C7	-63.9(3)
C1	N2	C2	C7	-178.9(2)	C10	C11	C12	N3	-0.8(3)
C1	C8	C9	C10	177.8(2)					

Table S7. Hydrogen Atom Coordinates (Å×10^4) and Isotropic Displacement Parameters (Å^2×10^3) for **1**.

Atom	x	y	z	U(eq)
H1	7975.43	4786.25	6024.72	41
H2	7362.73	1824.97	8319.12	28
H3	6682.48	3233.56	5491.5	26
H9	6000.44	1269.7	7440.38	34
H11	4301.9	1905.47	4982.92	32
H12	5379.53	3019.04	4510.78	31
H4A	9515.35	5096.84	7368.89	35
H4B	9849.75	3171.78	7382.24	35
H10	4624.93	987.93	6461.31	37
H5A	10700	4300.95	8713.59	44
H5B	9919.39	5240.45	8897.25	44
H7A	8999.29	1365.92	9491.91	40
H7B	8963.8	3388.52	9639.57	40
H6A	10380.5	2809.81	9844.15	45
H6B	10150.8	1605.37	8984.08	45
H2A	8130(20)	7340(40)	6645(12)	82(12)
H2B	7770(20)	7590(40)	5820(20)	131(19)

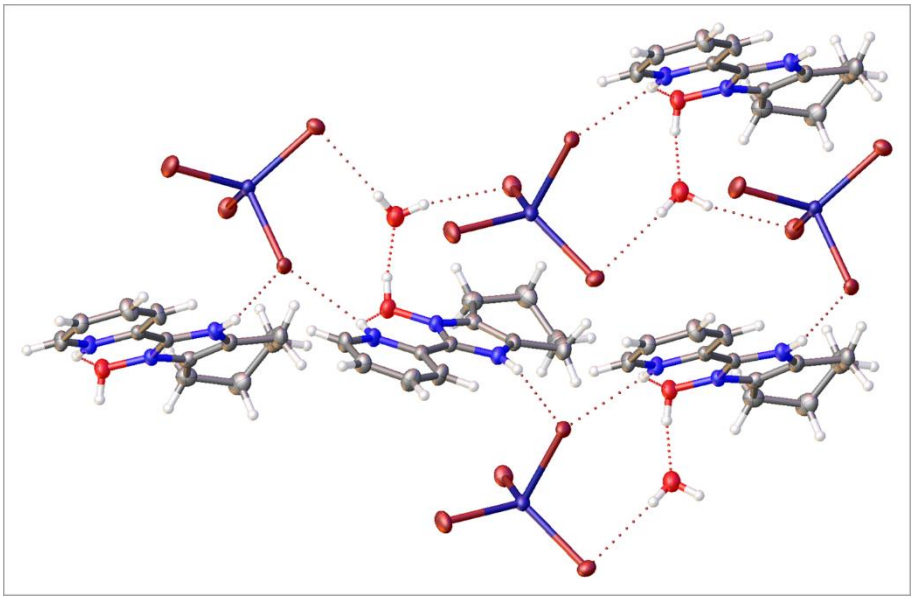

Figure S1. The structure of $[H_3L][MnBr_4][H_2O]$ moiety of **1** with hydrogen bonds presented by red lines.

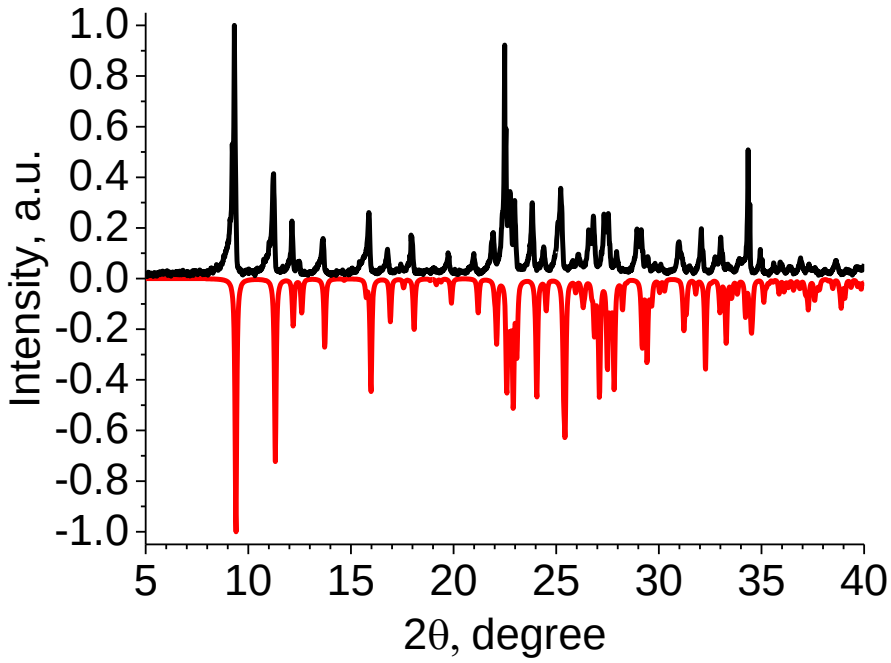

Figure S2. Comparison of experimental (black) XRPD patterns of **1** with the diffraction pattern, simulated for the crystal structure (red).

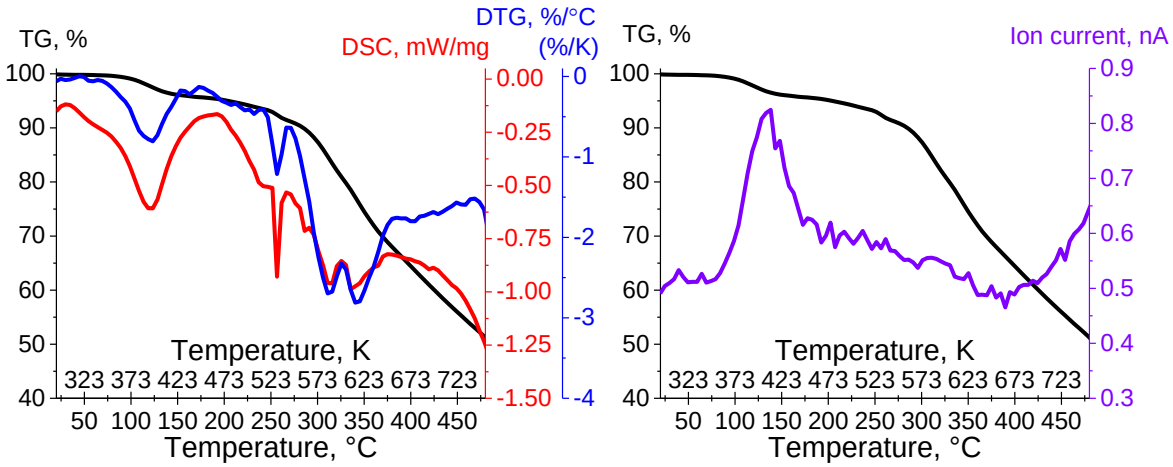

Figure S3. TG, DTG, and DSC curves (left) and TG with temperature dependence of the ion current of the mass spectrum at 18 Da (right) of **1**.

Table S8. TG, DTG, and DSC data of **1**.

Stage	Temperature range, °C (K)	Peak temperature, °C (K)	Mass loss, %	Fragment loss
1	80 – 150 (353 – 423)	120 (393)	3.5	H_2O
2	200 – 370 (473 – 643)	310 (583) and 340 (613)	27	HBr, HBr
3	370 – …(643 –)	–	–	

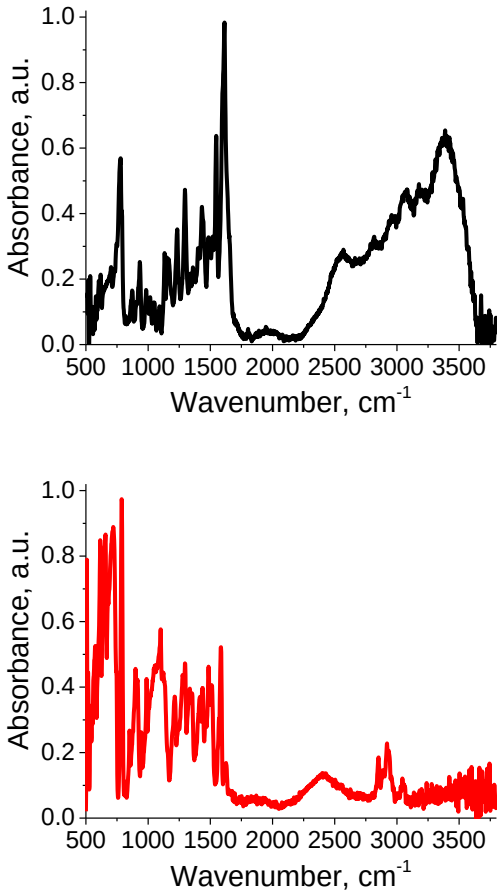

Figure S4. Experimental IR spectrum of **1** (top) and HL (bottom).

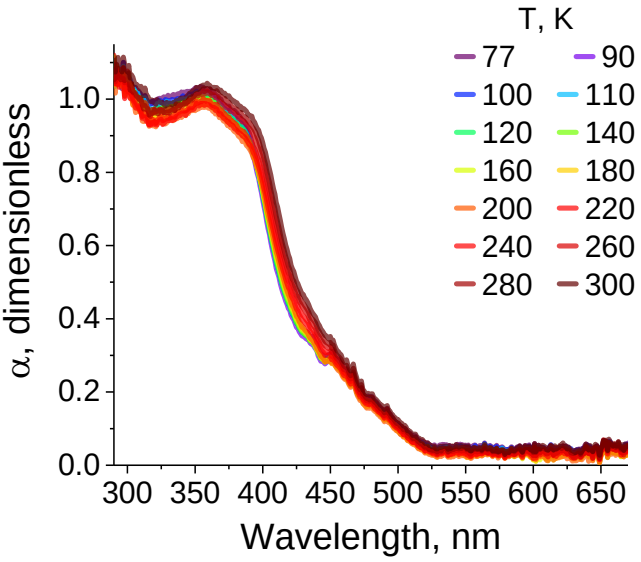

Figure S5. Temperature dependence of the absorption plot of **1**.

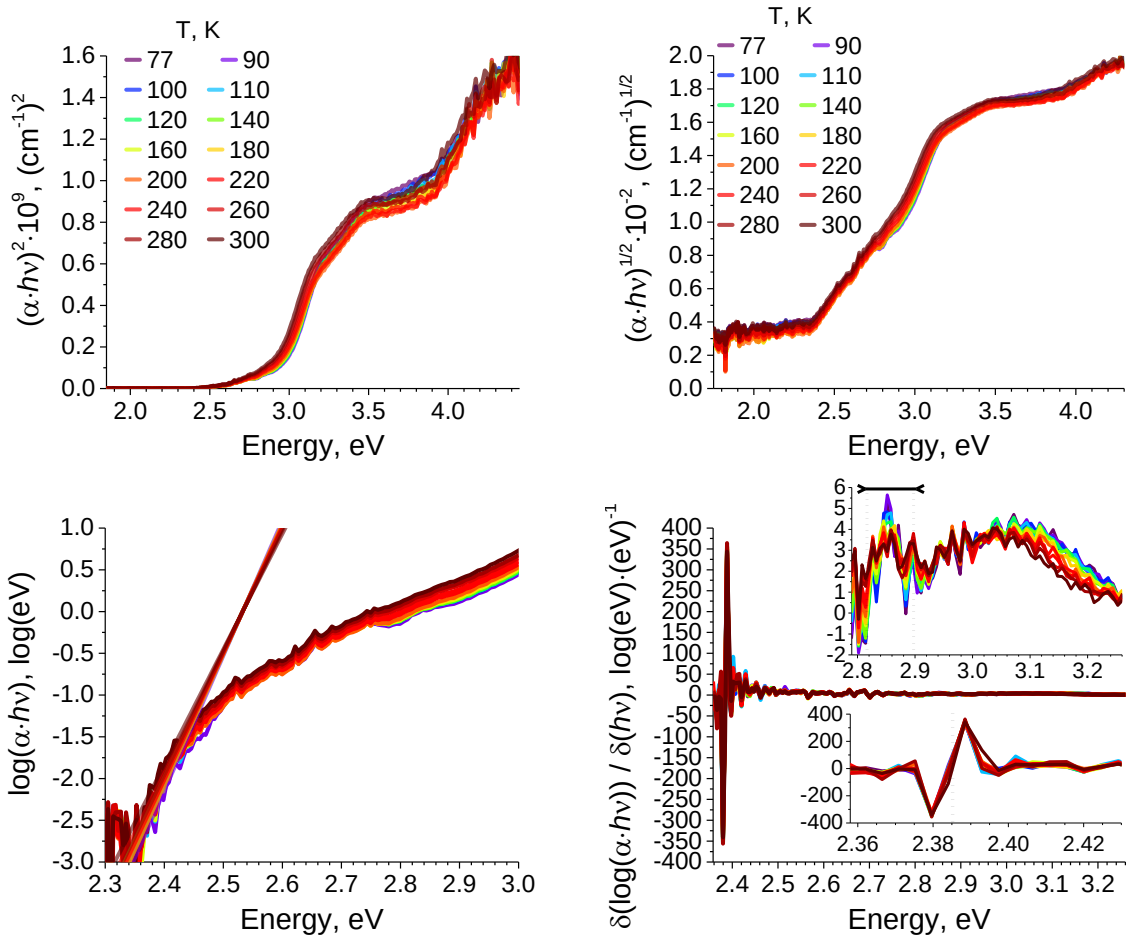

Figure S6. Temperature dependences of the Tauc plot of **1** (top). Temperature dependences of the $\log(\alpha \cdot h\vartheta)$ (bottom, left) with linear approximation corresponding to the Urbach energy calculation. The analysis of the indirect band gap of **1** $\frac{\delta(\log(\alpha\cdot h\vartheta))}{\delta(h\vartheta)}$ (bottom, right).

Footnote 1 for Figure S6. Spectrum near the onset of absorption can be described by the following equation:

$$\alpha \cdot h\vartheta = \alpha_0 \cdot \exp(\frac{h\vartheta - E_2^{indir}}{E_u}) \text{ or } \log(\alpha \cdot h\vartheta) = \log(\alpha_0) + \frac{h\vartheta - E_2^{indir}}{E_u}$$

where α_0 is a pre-exponential parameter, E_u is the temperature dependent Urbach Energy with E_u value for **1** increasing from 63 meV to 75 meV when temperature increase from 77 K to 300 K, and E_2^{indir} is the band-band transition energy $E_2^{indir} \approx 2.54$ meV.

Footnote 2 for Figure S6. Absorption spectrum of the indirect band-band transition can be described by the following equation:

$$\alpha \cdot h\vartheta \sim \frac{\left(h\vartheta - E_2^{indir} - E_p^{indir}\right)^2}{\exp\left(\frac{E_p^{indir}}{k_B * T}\right) - 1} + \frac{(h\vartheta - E_2^{indir} + E_p^{indir})^2}{1 - \exp\left(-\frac{E_p^{indir}}{k_B * T}\right)}$$

or

$$\log(\alpha \cdot h\vartheta) \sim \log(\frac{\left(h\vartheta - E_2^{indir} + E_p^{indir}\right)^2}{\exp\left(\frac{E_p^{indir}}{k_B * T}\right) - 1} + \frac{\left(h\vartheta - E_2^{indir} - E_p^{indir}\right)^2}{1 - \exp\left(-\frac{E_p^{indir}}{k_B * T}\right)})$$

The derivative of the logarithm of the absorption spectrum equals to:

$$\frac{\delta(\log(\alpha \cdot h\vartheta))}{\delta(h\vartheta)} \sim \frac{\delta(\log(\frac{\left(h\vartheta - E_2^{indir} + E_p^{indir}\right)^2}{\exp\left(\frac{E_p^{indir}}{k_B * T}\right) - 1} + \frac{\left(h\vartheta - E_2^{indir} - E_p^{indir}\right)^2}{1 - \exp\left(-\frac{E_p^{indir}}{k_B * T}\right)}))}{\delta(h\vartheta)}$$

$$\frac{\delta(\log(\alpha \cdot h\vartheta))}{\delta(h\vartheta)} \sim$$

$$2\frac{\left(1-\exp\left(-\frac{E_p^{indir}}{k_B * T}\right)\right)^{-1}\left(h\vartheta - E_2^{indir} - E_p^{indir}\right) + \left(\exp\left(\frac{E_p^{indir}}{k_B * T}\right) - 1\right)^{-1}\left(h\vartheta - E_2^{indir} + E_p^{indir}\right)}{\left(1-\exp\left(-\frac{E_p^{indir}}{k_B * T}\right)\right)^{-1}\left(h\vartheta - E_2^{indir} - E_p^{indir}\right)^2 + \left(\exp\left(\frac{E_p^{indir}}{k_B * T}\right) - 1\right)^{-1}\left(h\vartheta - E_2^{indir} + E_p^{indir}\right)^2}$$

The derivative equals to zero ($\frac{\delta(\log(\alpha \cdot h\vartheta))}{\delta(h\vartheta)} = 0$) at $h\vartheta =$

$$\frac{\left(1-\exp\left(-\frac{E_p^{indir}}{k_B * T}\right)\right)^{-1}\left(E_2^{indir} + E_p^{indir}\right) + \left(\exp\left(\frac{E_p^{indir}}{k_B * T}\right) - 1\right)^{-1}\left(E_2^{indir} - E_p^{indir}\right)}{\left(1-\exp\left(-\frac{E_p^{indir}}{k_B * T}\right)\right)^{-1} + \left(\exp\left(\frac{E_p^{indir}}{k_B * T}\right) - 1\right)^{-1}}.$$

For the $E_p^{indir} >> k_B * T$ ($E_p^{indir} >>$ 26 meV) the equation can be simplified to:

$$h\vartheta = E_2^{indir} + E_p^{indir}.$$

Assuming E_p^{indir} = 0, the equation can be simplified to:

$$h\vartheta = E_2^{indir}.$$

If the Urbach Energy is not zero, the E_2^{indir} is equal to $E_2^{indir} = \tilde{E}_2^{indir}\big|_{observed} + 2 * E_u$. Taking into account the Urbach Energy, the numerical solve of equations gives following values of E_2^{indir} and E_p^{indir}:

$h\vartheta = E_2^{indir} - 2 * E_u \rightarrow 2.39\ eV = E_2^{indir} - 2 * 0.075\ eV \rightarrow E_2^{indir} = 2.54\ eV$ and

$h\vartheta = E_2^{indir} + E_p^{indir} \rightarrow 2.85\ eV = 2.54\ eV + E_p^{indir} \rightarrow E_p^{indir} = 0.31\ eV$.

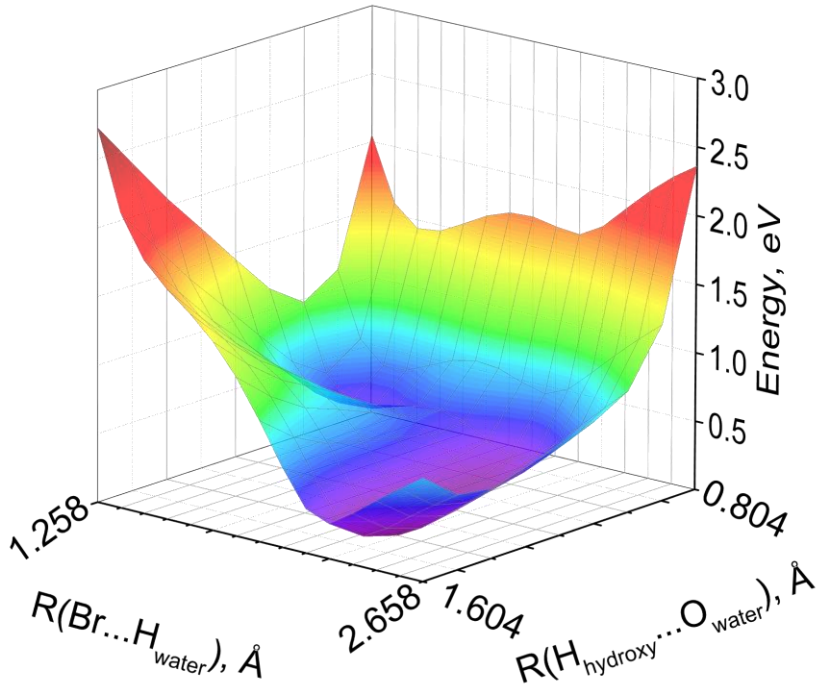

Figure S7. Calculated ground state potential energy surface of **1**.

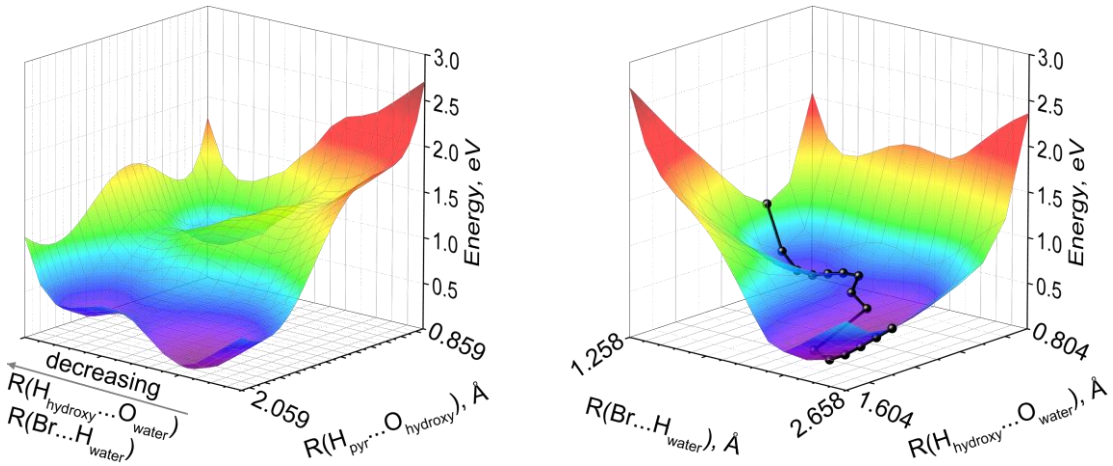

Figure S8. Calculated ground state potential energy surface along the $H_{pyr}…O_{hydroxy}$ distance changing corresponding the keto-enol tautomerization (left) and calculated ground state potential energy surface along the $Br…H_{water}$ and $H_{hydroxy}…O_{water}$ distance changing (right) showing the path for calculated keto-enol tautomerization energy potential surface of **1**.

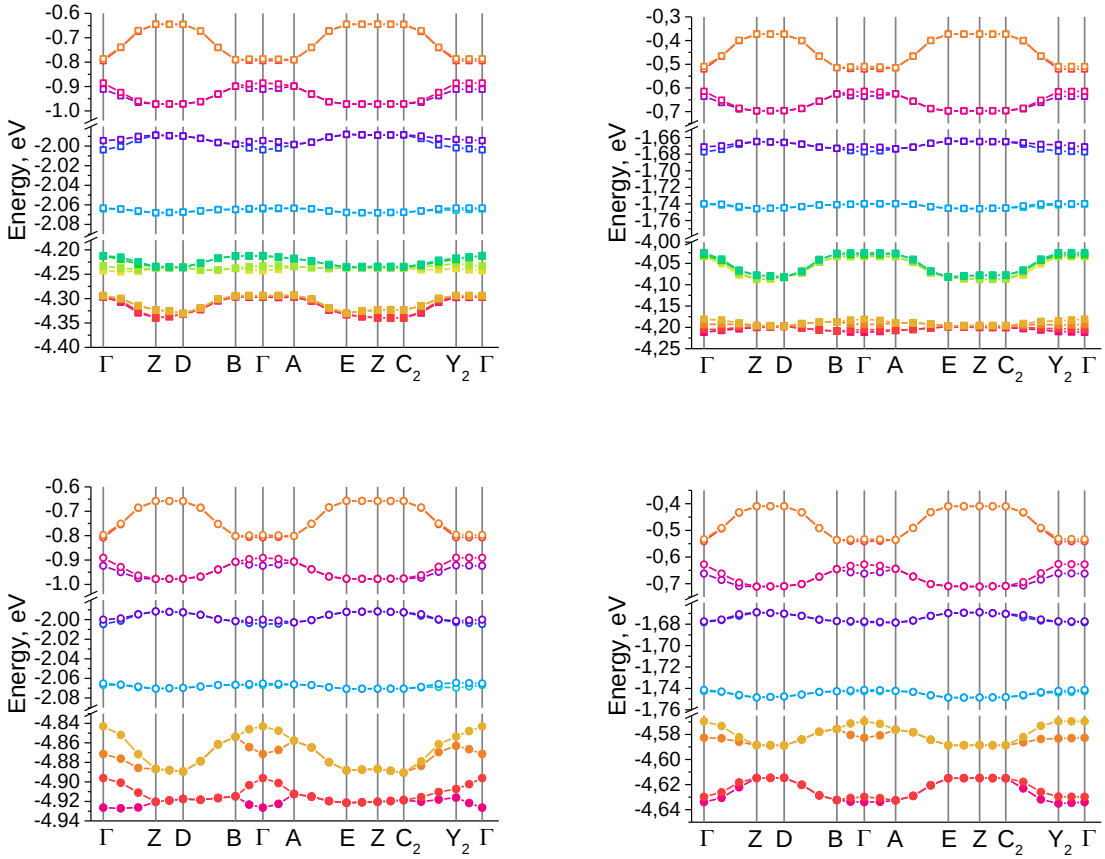

Figure S9. Calculated band structure for spin-up (top) and spin-down (bottom) of **1** in global (left) and local (right) minima.

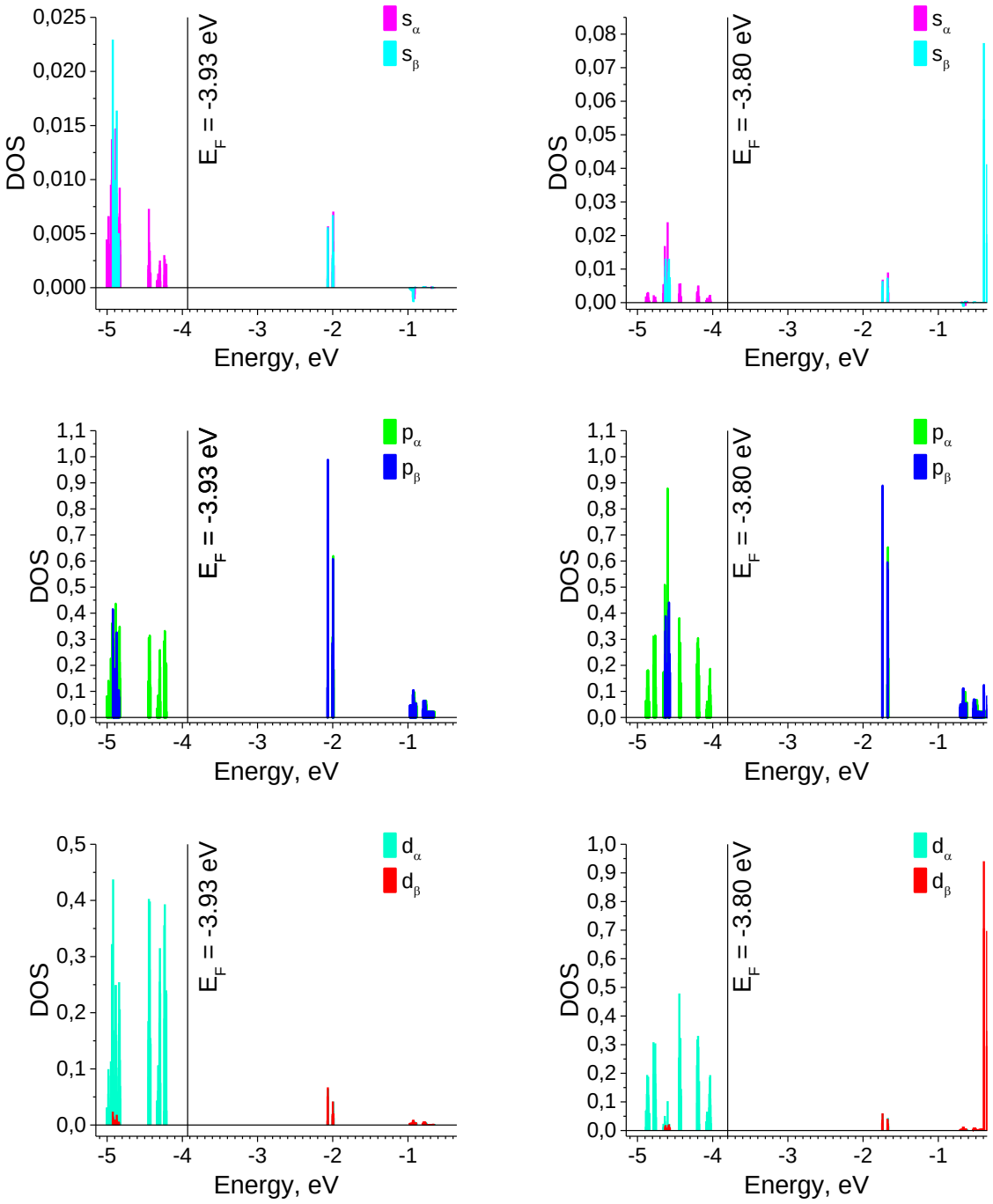

Figure S10. Calculated spin-up (α) and spin-down (β) DOS of **1** in global (left) and local (right) minima.

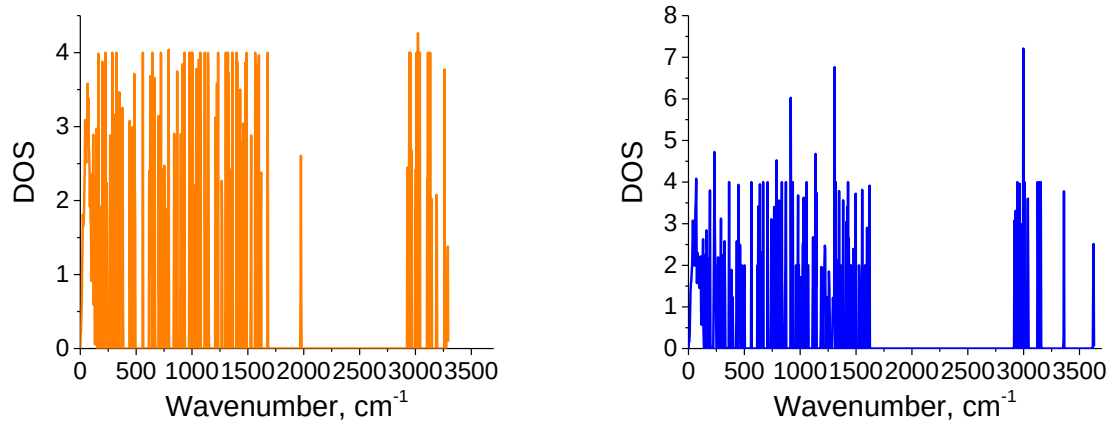

Figure S11. Calculated phonon energies of **1** in global (orange) and local (blue) minima.

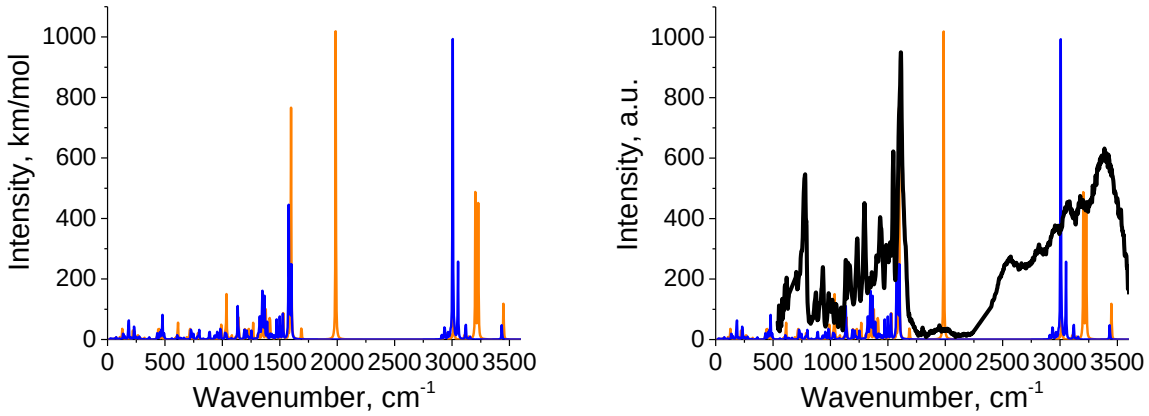

Figure S12. Calculated IR spectra of $[H_3L][MnBr_4][H_2O]$ fragments of **1** in global (orange) and local (blue) minima (left) and comparison with the experimental IR spectrum (right).

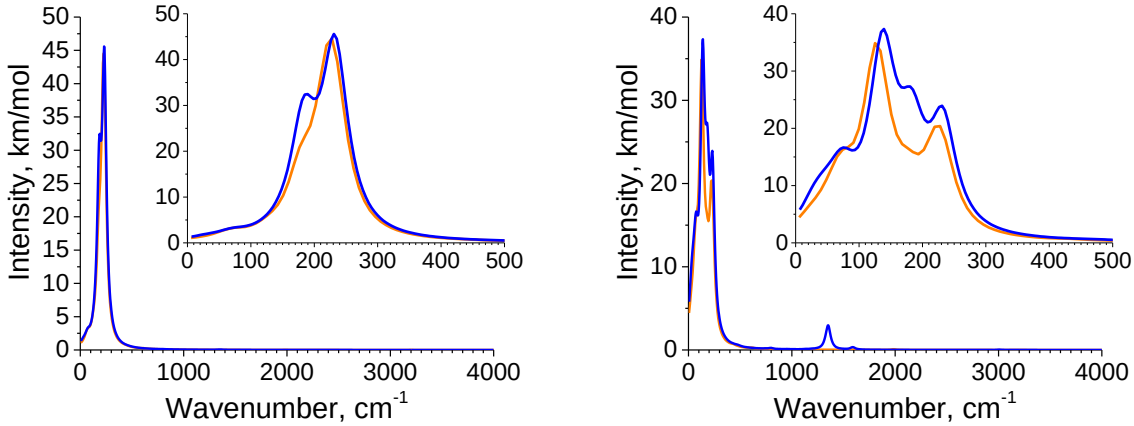

Figure S13. Calculated partial IR spectra of $[H_3L][MnBr_4][H_2O]$ fragments of **1** in global (orange) and local (blue) minima for manganese(II) ion (left) and four bromides (right).

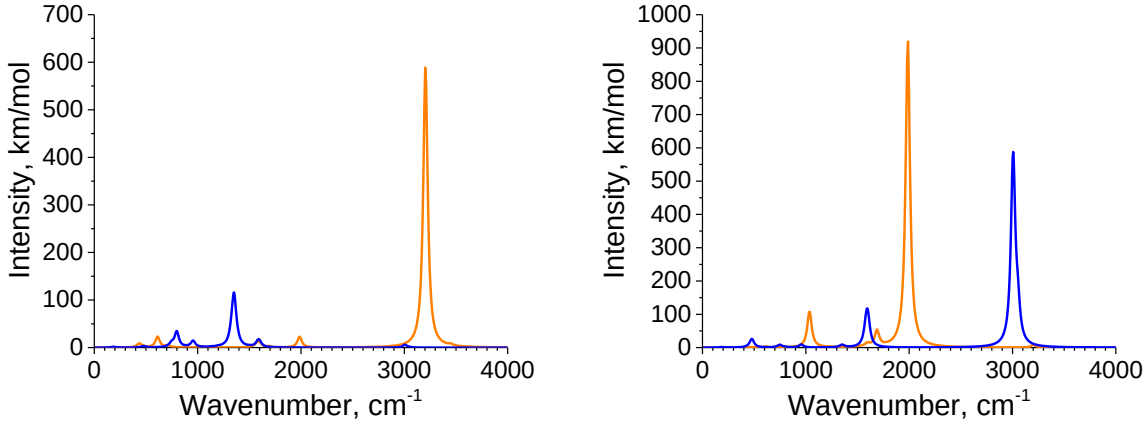

Figure S14. Calculated partial IR spectra of $[H_3L][MnBr_4][H_2O]$ fragments of **1** in global (orange) and local (blue) minima for proton of {Br…HO} (left) and {O…HO} (right) fragments.

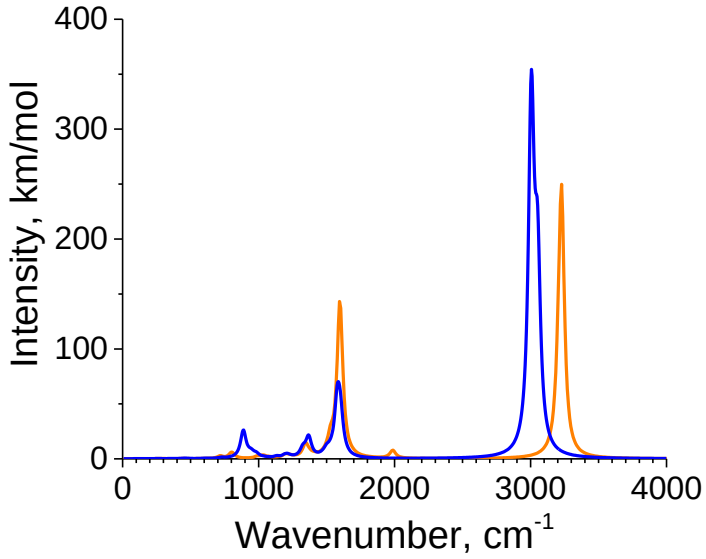

Figure S15. Calculated partial IR spectra of $[H_3L][MnBr_4][H_2O]$ fragments of **1** in global (orange) and local (blue) minima for proton of {N…HO} fragment.

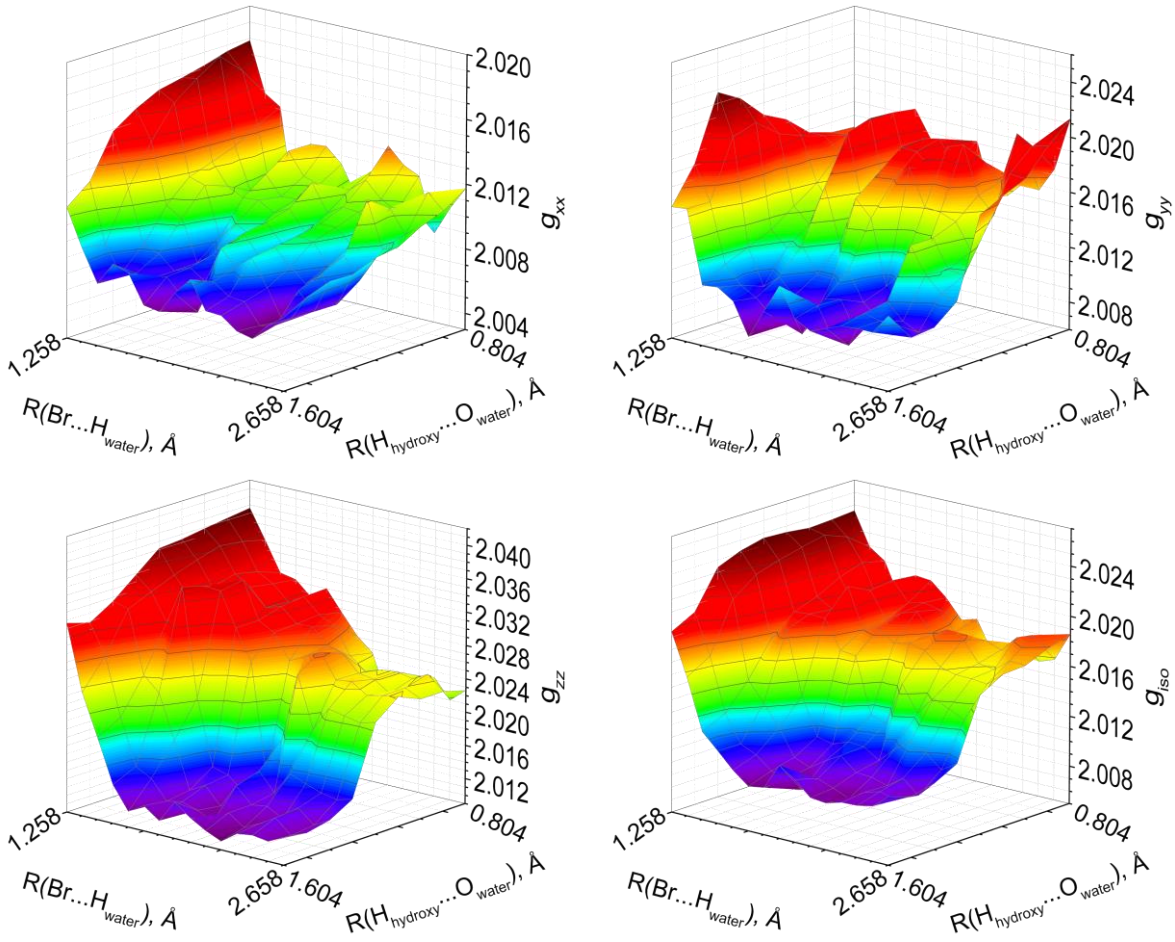

Figure S16. Calculated ***g*** –tensor values along the ground state potential energy surface of **1**.

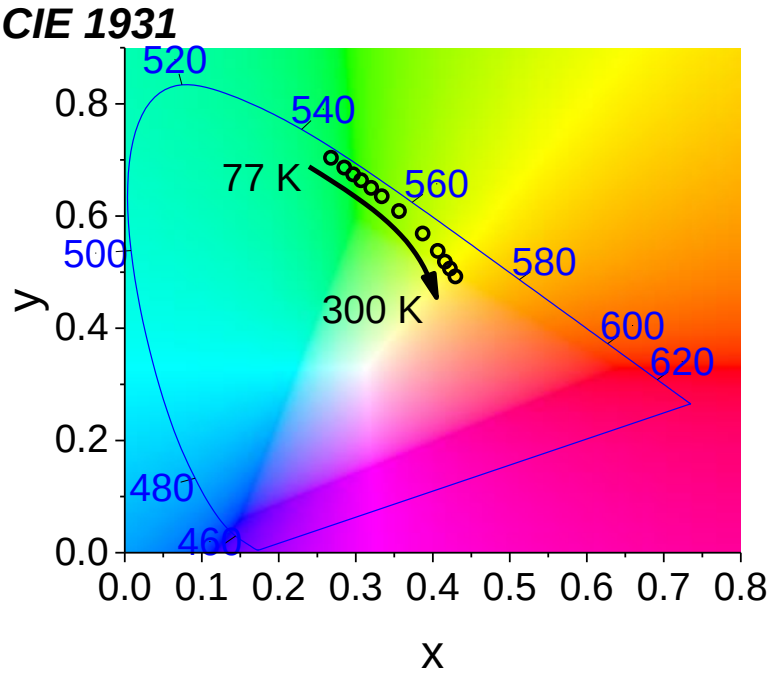

Figure S17. Temperature dependences of the photoluminescence chromaticity of **1** (λ_{Ex} = 455 nm).

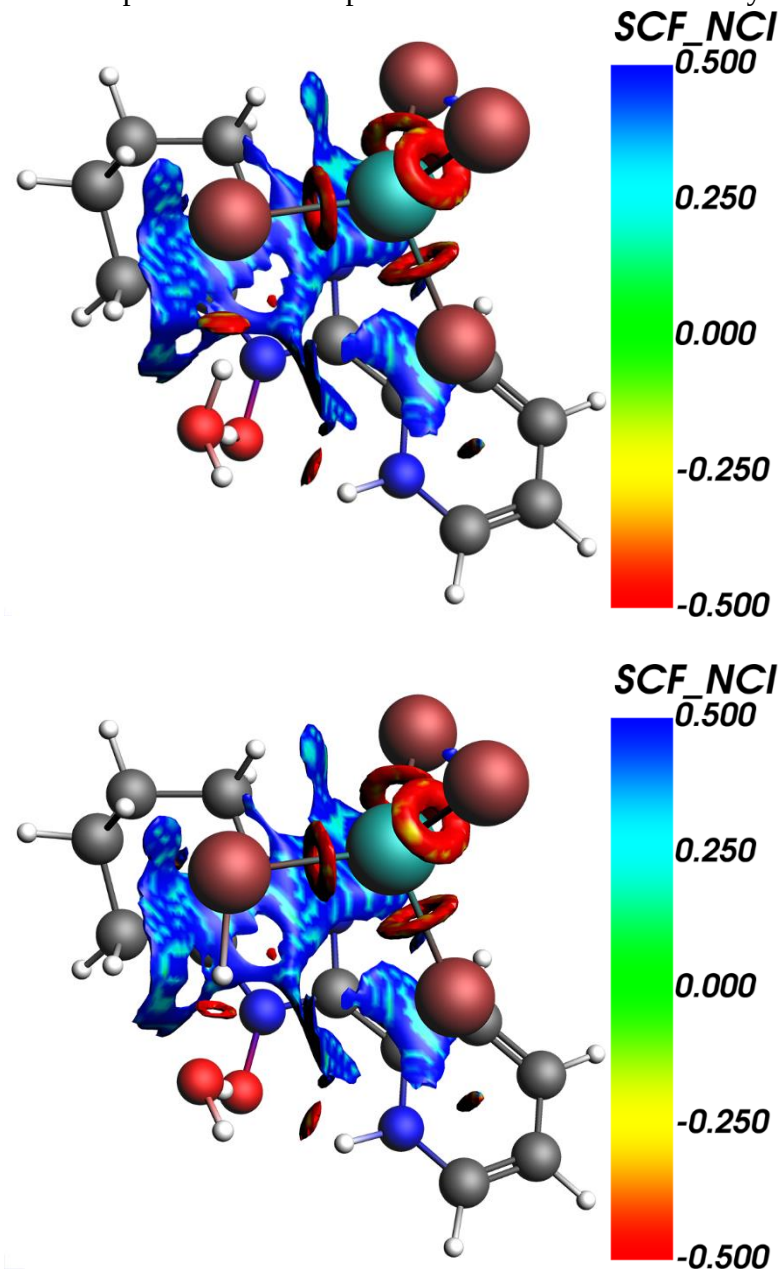

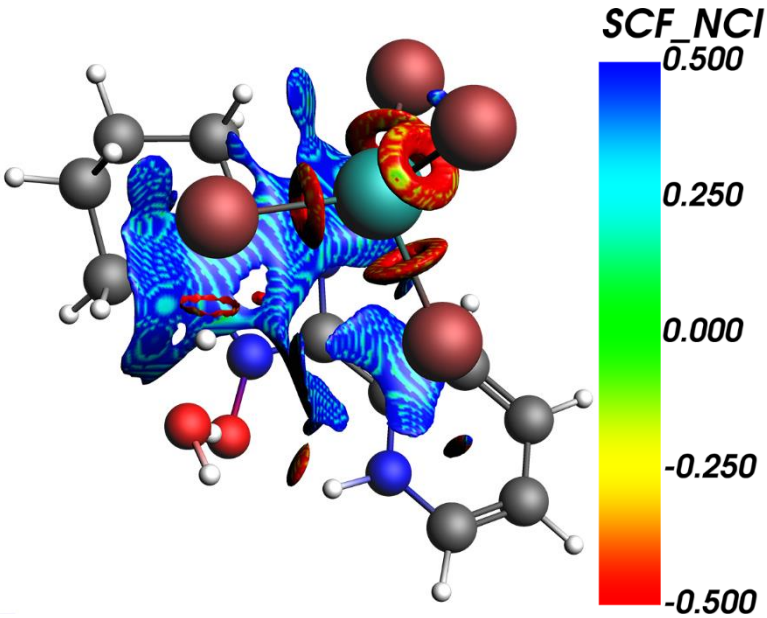

Figure S18. The noncovalent interaction (NCI) plots for **1** showing different RH…Br(Mn) interactions. NCIs (SCF density) are presented by isosurfaces (s = 0.5 a.u., ρ= 0.02 a.u.) colored according to sign(λ_2)ρ in the red-green-blue scheme (top – global minimum PES, center – local minimum PES, bottom – mediate state between global and local minima PES).

The Hirshfeld surfaces and fingerprint plot were calculated using CrystalExplorer program version 21.5 [1].

1. Spackman, P. R., Turner, M. J., McKinnon, J. J., Wolff, S. K., Grimwood, D. J., Jayatilaka, D., Spackman, M. A. CrystalExplorer: a program for Hirshfeld surface analysis, visualization and quantitative analysis of molecular crystals. *J. Appl. Cryst.* **2021,** *54*, 3, 1006–1011, doi: 10.1107/S1600576721002910.

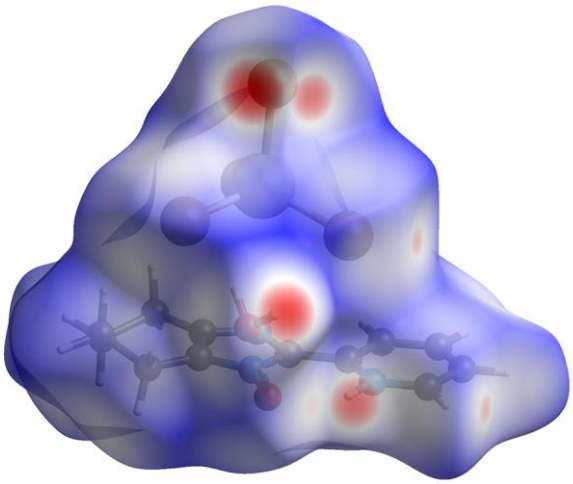

Figure S19. The Hirshfeld surface for the $[H_3L][MnBr_4][H_2O]$ in the crystal **1** mapped with d_{norm}.

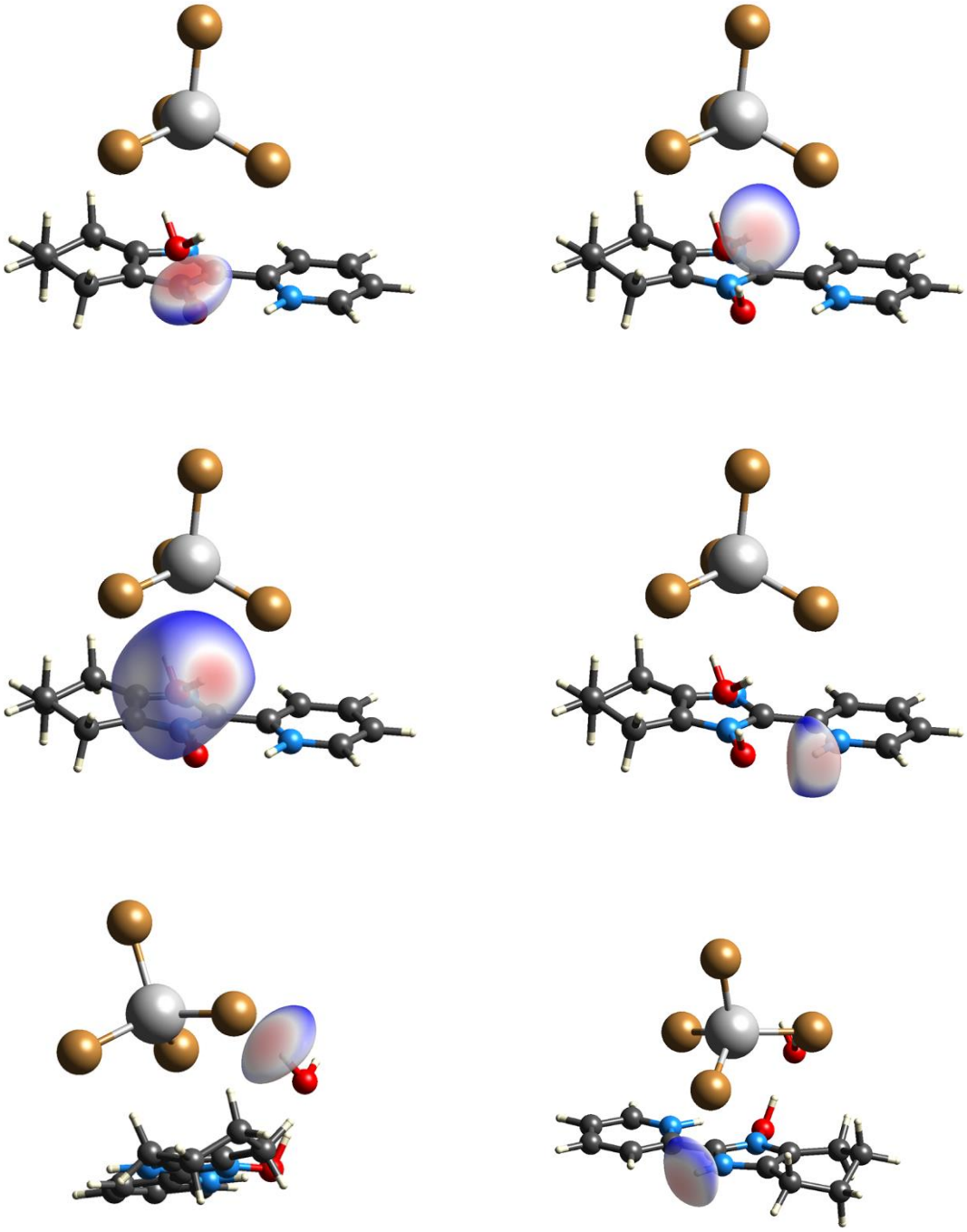

Figure S20. The Hirshfeld surfaces for the different protons in the crystal **1** mapped with d_{norm}.

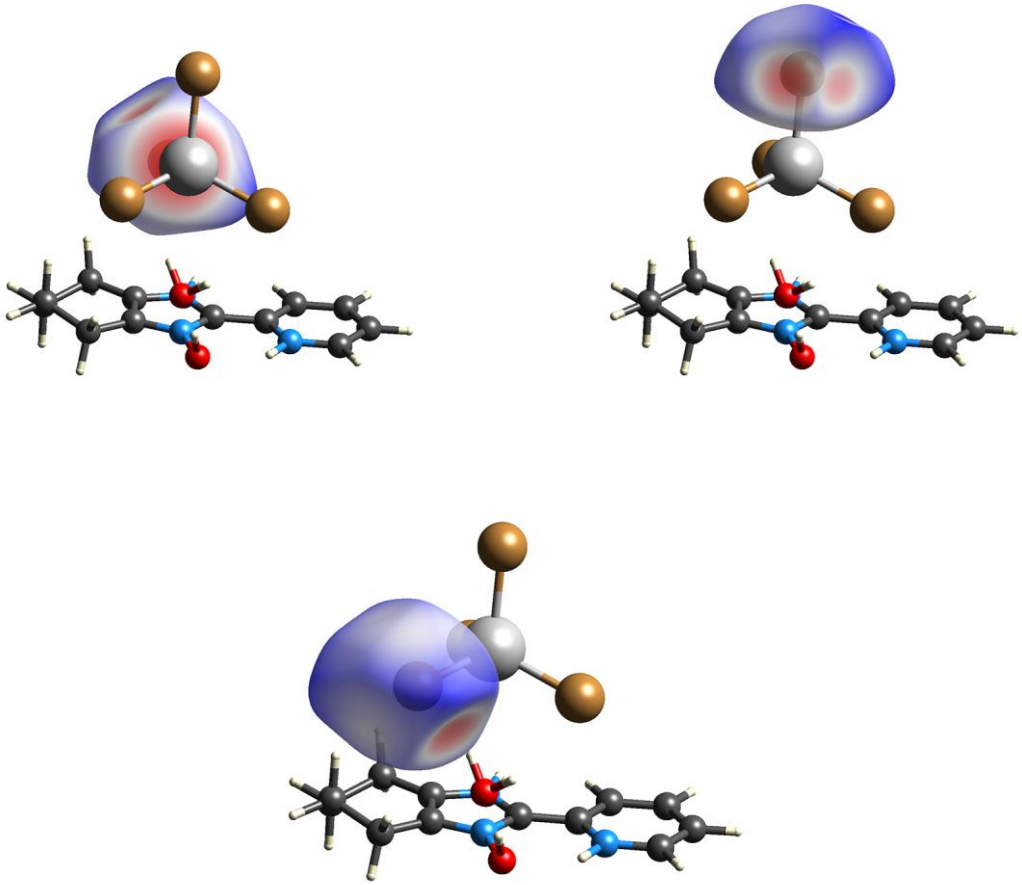

Figure S21. The Hirshfeld surfaces for the bromides in the crystal **1** mapped with d_{norm}.

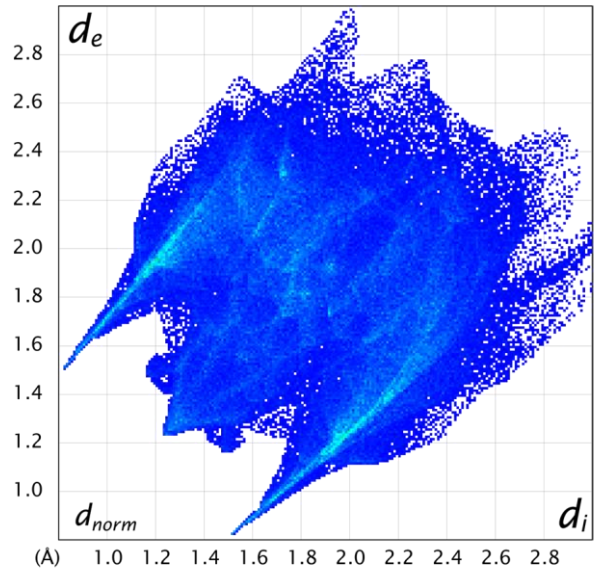

Figure S22. Fingerprint plot for the $[H_3L][MnBr_4][H_2O]$ in the crystal **1**. Surface volume is 481.96 $Å^3$, surface area is 379.93 $Å^2$, surface asphericity is 0.031, and surface globularity is 0.782.

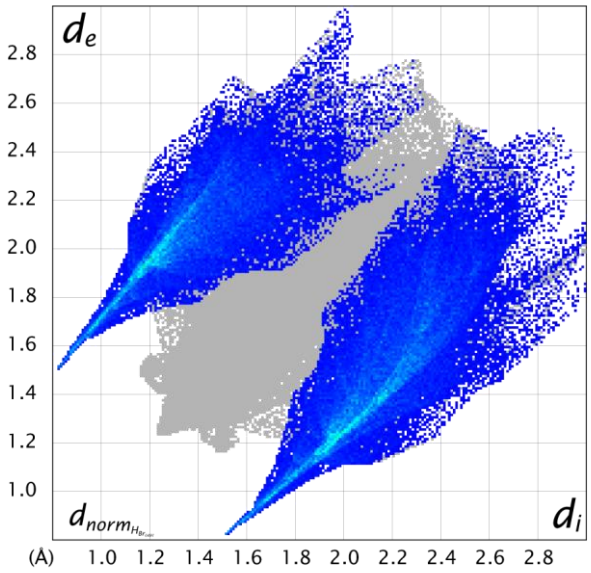

Figure S23. Fingerprint plot for the $[H_3L][MnBr_4][H_2O]$ in the crystal **1**. The H…Br close contacts show (surface area – 49.1 %).

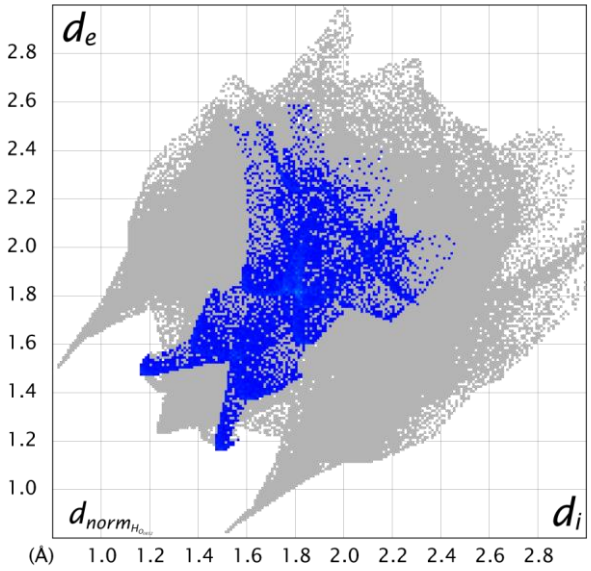

Figure S24. Fingerprint plot for the $[H_3L][MnBr_4][H_2O]$ in the crystal **1**. The H…O close contacts show (surface area – 5.2 %).

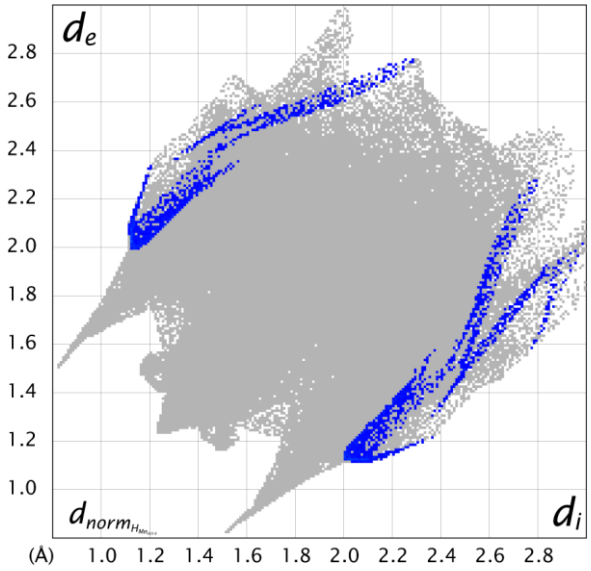

Figure S25. Fingerprint plot for the $[H_3L][MnBr_4][H_2O]$ in the crystal **1**. The H…Mn close contacts show (surface area – 1.4 %).

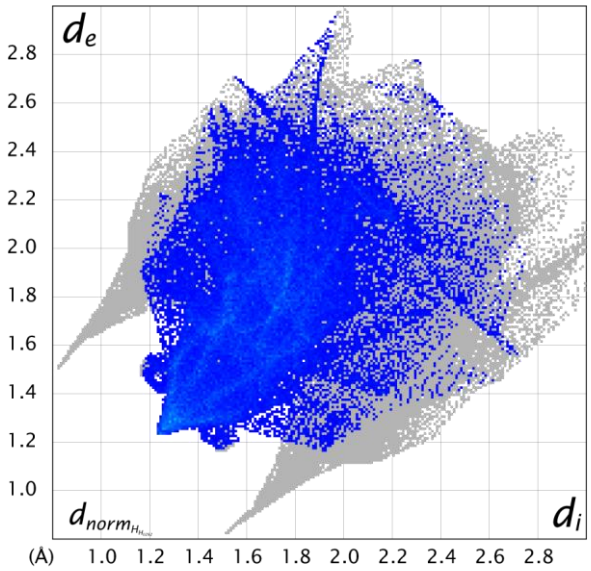

Figure S26. Fingerprint plot for the $[H_3L][MnBr_4][H_2O]$ in the crystal **1**. The H…H close contacts show (surface area – 29.2 %).

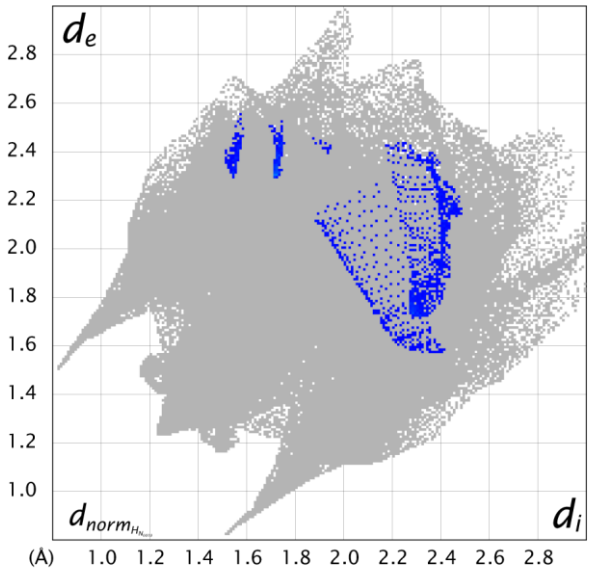

Figure S27. Fingerprint plot for the $[H_3L][MnBr_4][H_2O]$ in the crystal **1**. The H…N close contacts show (surface area – 1.0 %).

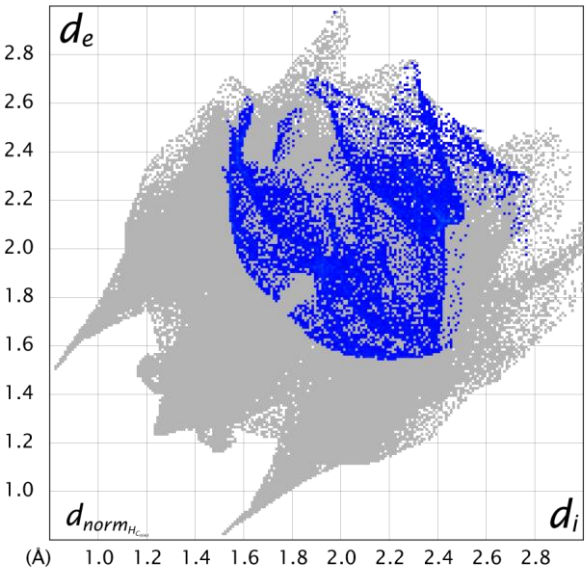

Figure S28. Fingerprint plot for the $[H_3L][MnBr_4][H_2O]$ in the crystal **1**. The H…C close contacts show (surface area – 6.3 %).